

## CLASSICAL Oe STARS IN THE FIELD OF THE SMALL MAGELLANIC CLOUD\*

JESSE B. GOLDEN-MARX<sup>1</sup>, M. S. OEY<sup>1</sup>, J. B. LAMB<sup>2</sup>, ANDREW S. GRAUS<sup>3</sup>, AARON S. WHITE<sup>1</sup>

\*\*\* Accepted in ApJ \*\*\*

## ABSTRACT

We present  $29 \pm 1$  classical Oe stars from RIOTS4, a spatially complete, spectroscopic survey of Small Magellanic Cloud (SMC) field OB stars. The two earliest are O6e stars, and four are earlier than any Milky Way (MW) Oe stars. We also find ten Ope stars, showing He I infill and/or emission; five appear to be at least as hot as  $\sim$ O7.5e stars. The hottest, star 77616, shows He II disk emission, suggesting that even the hottest O stars can form decretion disks, and offers observational support for theoretical predictions that the hottest, fastest rotators can generate He<sup>+</sup>-ionizing atmospheres. Our data also demonstrate that Ope stars correspond to Oe stars earlier than O7.5e with strong disk emission. We find that in the SMC, Oe stars extend to earlier spectral types than in the MW, and our SMC Oe/O frequency,  $0.26 \pm 0.04$ , is much greater than the MW value,  $0.03 \pm 0.01$ . These results are consistent with angular momentum transport by stronger winds suppressing decretion disk formation at higher metallicity. In addition, our SMC field Oe star frequency is indistinguishable from that for clusters, which is consistent with the similarity between rotation rates in these environments, and contrary to the pattern for MW rotation rates. Thus, our findings strongly support the viscous decretion disk model and confirm that Oe stars are the high-mass extension of the Be phenomenon. Additionally, we find that Fe II emission occurs among Oe stars later than O7.5e with massive disks, and we revise a photometric criterion for identifying Oe stars to  $J - [3.6] \geq 0.1$ .

*Subject headings:* galaxies: stellar content — stars: circumstellar matter — stars: early-type — stars: emission-line, Be — stars: evolution — stars: rotation

## 1. INTRODUCTION

Despite their scarcity and short lifespans, massive stars shape the evolution of their host galaxies through strong stellar winds and radiative feedback, which shock heat and ionize the surrounding gas, injecting energy into the interstellar medium (ISM). Moreover, when massive stars end their lives as core-collapse supernovae, the shock-waves can trigger or suppress star formation while enriching the ISM with metals. Thus, distinct types of feedback are associated with different evolutionary phases of massive stars. Understanding massive star evolution is complex due in part to the effects of mass loss and the difficulty of modeling their atmospheres, which cannot be treated as being in LTE. Recent stellar evolution models show that properties such as rotation and binarity also strongly affect massive star evolution. According to models by Ekström et al. (2012), rapid rotation induces rotational mixing, which increases the time these stars spend on the main sequence by continually replenishing their cores with H. Thus, rapid rotation increases the main sequence lifetimes of massive stars and allows them to emit more H-ionizing photons at later times in their evolution (e.g., Levesque et al. 2012). Binarity is also key, since observations suggest that the majority of massive stars are binaries (e.g., Sana et al. 2014), and de Mink et al. (2013) suggest that binary interactions

increase the rotation rates of  $\sim$ 20% of massive stars.

Understanding different types of evolved massive stars may offer clues about the physical processes that drive their evolution. Classical Be stars are apparently a subclass of somewhat evolved massive stars whose formation depends on rapid rotation and possibly on binarity. Today, classical Be stars are characterized as rapidly rotating, non-supergiant B stars with spectra containing Balmer emission lines, which are often double peaked (e.g., Collins 1987; Rivinius et al. 2013), resulting from Keplerian rotation of a circumstellar disk (e.g., Struve 1931). In addition to the Balmer emission, Be star spectra can show three types of variability (McLaughlin 1961): Balmer line variability; variation in the ratio of the violet and red components of the double-peaked Balmer emission lines, or V/R variability; and the appearance or disappearance of a narrow Balmer absorption core, known as a shell absorption spectrum (e.g., Hanuschik 1996).

Struve (1931) presented the first viable Be star model, which proposed that the circumstellar disks surrounding Be stars form when the stellar rotation rate  $v_{\text{rot}}$  approaches the critical velocity  $v_{\text{crit}}$ , where the gravitational and centrifugal forces are equal, causing the centrifugal force to eject the equatorial layer into a disk. Struve's model omits stars whose spectra contain P Cygni profiles because Balmer emission from classical Be stars originates from a circumstellar disk, not an isotropic wind, emphasizing that rapid rotation is the primary cause of the Be phenomenon.

Although Struve's model served as the foundation for understanding Be stars, observations suggest that on average, Be stars rotate at only  $\sim 0.80 v_{\text{crit}}$  (e.g., Rivinius et al. 2006; Meilland et al. 2012; Chauville et al. 2001).

\* This paper includes data gathered with the 6.5 meter Magellan Telescopes located at Las Campanas Observatory, Chile.

<sup>1</sup> Department of Astronomy, University of Michigan, 1085 S. University Ave, Ann Arbor, MI, 48109-1107; jessegm@umich.edu

<sup>2</sup> Department of Physical Sciences, Nassau Community College, One Education Drive Garden City, NY, 11530-6793

<sup>3</sup> Department of Physics and Astronomy, University of California at Irvine, Irvine, CA, 92697-4575

However, gravitational limb darkening may cause these rotational rates to be underestimated (e.g., Stoeckley 1968; Townsend et al. 2004; Frémat et al. 2005), thus suggesting that Be stars may rotate closer to  $v_{\text{crit}}$  than observations find. Determining how Be stars form with subcritical rotation rates led to the viscous decretion disk model (VDD; Lee et al. 1991). This model proposes that processes such as non-radial pulsation (NRP) spin up the stellar atmosphere to slightly super-Keplerian rotation speeds and that if the outer layers are continually supplied with angular momentum, they are lifted from the star and move into a disk (e.g., Lee et al. 1991; Porter 1999). These viscous disks are characterized by outward angular momentum transfer due to a turbulent viscosity and resemble models for accretion disks, but with angular momentum supplied at the inner boundary of the disk (Lee et al. 1991). Interferometric observations and observations of V/R and photometric variability from the disk support the VDD model and its predictions (e.g., Rivinius et al. 2013).

Currently, NRPs are the favored mechanism for ejecting sub-critically rotating circumstellar material into a Keplerian orbit. NRPs require  $\Delta v = v_{\text{crit}} - v_{\text{rot}}$  to be approximately equal to the pulsation amplitude, which for NRPs can approach or slightly exceed the sound speed (Owocki 2006). Therefore, NRPs require the star to rotate close to  $v_{\text{crit}}$ . However, for some Be stars with slower  $v_{\text{rot}}$ , NRPs may be unable to eject the material and form decretion disks, so the mechanism for transporting material to the disk remains an open question.

Regardless of ejection mechanism, the VDD model requires Be stars rotate near  $v_{\text{crit}}$  to form decretion disks. Stellar evolution models demonstrate that as isolated stars evolve, the surface rotation velocity,  $v_{\text{rot}}$ , can approach  $v_{\text{crit}}$ , even though  $v_{\text{rot}}$  decreases (e.g., Langer 1998; Meynet & Maeder 2003). The rotation rate,  $\Omega$ , also evolves towards the Keplerian limit if the star retains angular momentum while on the main sequence and transports it efficiently between its core and envelope (e.g., Negueruela et al. 2004; Ekström et al. 2008; de Mink et al. 2013). Additionally, binary interactions have been proposed to spin-up Be stars to  $v_{\text{crit}}$ . McSwain & Gies (2005) suggest that binary interactions may be involved in spinning up as many as 73% of Be stars; however much debate exists about the role of binarity in forming Be stars.

One way to evaluate the VDD model is to study Oe stars, first identified by Conti & Leep (1974) and proposed as an early-type extension of the Be phenomenon due to He II absorption and Balmer emission. Conti & Leep (1974) defined Oe stars as rapidly rotating O stars with spectra containing Balmer emission, but not the characteristic Of star emission features, He II  $\lambda 4686$  and N III  $\lambda\lambda 4634\text{--}40\text{--}42$ , associated with strong stellar winds. Oe stars also show additional characteristics similar to classical Be stars, including V/R and Balmer line variability (Divan et al. 1983; Rauw et al. 2007) and in some cases, He I emission (e.g., Frost & Conti 1976). However, polarization measurements from Vink et al. (2009) have not been able to confirm that circumstellar disks surround Oe stars. Thus, there is still some uncertainty that Oe stars are the high-mass analogs of the Be phenomenon.

There is another rare class of O stars which has also

been proposed to correspond to higher-mass analogs of the Be phenomenon, the Onfp (Walborn 1973) or Oef (Conti & Leep 1974) stars. These are O stars with double-peaked He II  $\lambda 4686$  emission. However, unlike Oe stars, Onfp stars show Balmer emission only in H $\alpha$  (Conti & Leep 1974). Furthermore, while double-peaked He II  $\lambda 4686$  emission may suggest a disk, more recently, this emission has been proposed to come from stellar winds (e.g., Walborn et al. 2010). The status of Onfp stars remains uncertain, and Oe stars are generally considered to be the early-type analogs to Be stars. However, there have been few studies of Oe stars as a class. The study with the largest sample to date is by Negueruela et al. (2004), who took new spectra of all previously identified Oe, emission-line O, and peculiar O stars in the Milky Way (MW) visible from La Palma Observatory.

O stars have stronger winds than B stars, so the frequency of Oe relative to Be stars should provide a critical probe of the VDD model. Since stellar wind strength increases with stellar mass and metallicity, in high-metallicity environments, line-driven winds from higher-mass stars should remove angular momentum and inhibit rotation near  $v_{\text{crit}}$ , suppressing decretion disk formation among early-type stars. Negueruela et al. (2004) stress that the Galactic frequency of Oe stars is low, only  $0.04 \pm 0.02$  among O7.5 – O9 stars, based on the catalog of Maíz-Apellániz et al. (2004). We confirm an Oe/O ratio of  $0.03 \pm 0.01$ , where the denominator includes Oe and O stars, based on luminosity class III–V stars from the Galactic O Star Spectroscopic Survey (GOSSS; Sota et al. 2011, 2014a,b), a complete magnitude-limited survey of Galactic O stars with  $B < 8$ . We caution this Oe/O value may be underestimated if stars with weak Balmer emission are not identified; however, even if twice as many MW Oe stars exist, the frequency is far less than the observed Be/B ratio,  $0.17 \pm 0.03^5$  (Zorec & Briot 1997), for B stars in the MW field. Moreover, the change in frequency of the Be phenomenon between O and B stars is steep. The Be/B ratio is  $0.27 \pm 0.01$  for B0 stars in the MW field (Zorec & Briot 1997), far greater than  $0.05 \pm 0.03$ , the frequency for O9.5 stars in the MW (Sota et al. 2014b). Thus, these frequencies are qualitatively consistent with the expected effect of wind strength on decretion disk formation. Negueruela et al. (2004) point out that since O8–9 V stars are the progenitor population of B0–1 IIIe stars, the high frequency of Be stars among B0–1 III stars implies that  $\Omega/\Omega_{\text{crit}}$  must increase during the main sequence phase;  $\Omega_{\text{crit}}$ , the critical rotation rate, has a non-linear relation to  $v_{\text{crit}}$  (e.g. Chauville et al. 2001; Martayan et al. 2006a; Rivinius et al. 2013).

Metallicity, as well as stellar mass, affects stellar wind strength and the ability to form decretion disks. Existing data support this interpretation; in the low-metallicity Small Magellanic Cloud (SMC), on average, B stars rotate at  $0.58 \Omega_{\text{crit}}$ , which is much faster than in the MW, where B stars rotate at  $0.30\text{--}0.40 \Omega_{\text{crit}}$  (Martayan et al. 2007b). These observations are consistent with findings from Martayan et al. (2010) that the frequency of Oe/Be stars among early-type stars in the SMC is  $\sim 3\text{--}5$  times higher than in the MW. Measurements of the Be/B ratio

<sup>5</sup> No uncertainty is provided for this value. Based on the quoted errors for the frequencies of individual spectral types, the aggregate uncertainty is likely  $\lesssim 0.03$ . We henceforth adopt this value.

across all B spectral types are estimated to be between 0.20–0.40 in the SMC (Martayan et al. 2007a), while Zorec & Briot (1997) obtain a frequency of  $0.17 \pm 0.03$  in the MW field. In low-metallicity systems, the frequency of the Be phenomenon should also be enhanced among earlier-type OB stars. Reports of an SMC O7 Ve (Massey et al. 1995), an SMC O4–7e (Evans et al. 2004) star, and an O3e star (Conti et al. 1986) in the Large Magellanic Cloud (LMC) suggest that this may indeed be the case, since stars of such early types have not been found in the Galaxy (§ 4.1).

Additionally, metallicity impacts NRPs. Since the pulsational amplitude is approximately equal to  $\Delta v$ , in low-metallicity environments, where OB stars rotate faster, it should be easier for NRPs to drive decretion disk formation. Moreover, rapid rotation leads to rotational mixing, which enriches the metallicity in the outer layers of stars, enhancing NRPs (Maeder & Meynet 2001). Thus, the faster rotation in low-metallicity environments favors pulsation, explains the higher frequency of pulsating Be stars in low-metallicity environments (Diago et al. 2009), and supports the anticorrelation between metallicity and frequency of the Be phenomenon. While metallicity clearly impacts single Be star formation, it also affects binary Be star formation because in low-metallicity environments, the progenitor stars retain more angular momentum and rotate faster, making it easier for binary interactions to spin up the star towards  $v_{\text{crit}}$ .

Metallicity may not be the only environmental factor that influences OB star rotation rates and decretion disk formation. In the Galaxy, OB stars rotate more slowly in the field than in clusters (e.g., Guthrie 1984; Wolff et al. 2007, 2008). Field OB stars may rotate more slowly because they form in lower density environments characterized by lower turbulent velocities and lower infall rates than their cluster counterparts, resulting in the formation of stars with lower rotation rates (Wolff et al. 2007, 2008). Alternatively, field stars may be older, more evolved stars that have dispersed from their clusters and rotate more slowly because their radius and moment of inertia increase as they evolve (Huang & Gies 2008; Huang et al. 2010). Stellar winds also strip angular momentum from these stars, further slowing their rotation with age. If the observed slower rotation in the field is an age effect, these arguments offer possible explanations, although we earlier cited arguments that rotation rates increase, rather than decrease, with age. In any case, even in low-metallicity environments, if field OB stars are older, on average, the possibility exists that they may be less likely to rotate rapidly enough to form decretion disks. In any case, given the higher frequency of rapid rotators in clusters, we might therefore expect the Oe/Be star frequency to be higher in clusters. To date, few studies have observed how field and cluster environments affect decretion disk formation. Martayan et al. (2007a) measure the Be/B ratio in the SMC clusters to be 0.20–0.40 and  $0.26 \pm 0.04$  in the field surrounding NGC 330, yielding inconclusive results.

Although the frequency of Be stars has been studied in many environments, similar work on Oe stars is lacking, and few statistically complete spectroscopic samples of either Oe or Be stars exist. Here, we use the Runaways and Isolated O Type Star Spectroscopic Survey of the SMC (RIOTS4), a spatially complete spectroscopic

survey of SMC field OB stars (Lamb et al. 2015), to identify a complete sample of classical Oe stars in the SMC field. We obtain their spectral type distribution, measure their frequency, and evaluate the effects of metallicity and field environment. In what follows, we present  $29 \pm 1$  SMC field Oe stars, of which only two have previously been classified as Oe stars. There are also two O6e stars, the earliest unambiguous SMC Oe stars identified to date. Our observations demonstrate that Oe stars are the higher-mass analogs of the Be phenomenon, clarify the relationship between Ope stars and Oe stars, and reveal observational support for recent stellar evolution models of hot, rapidly rotating stars.

## 2. THE RIOTS4 SURVEY

RIOTS4 is a spatially complete, spectroscopic survey targeting 374 photometrically selected SMC field OB stars (Lamb et al. 2015), identified from Oey et al. (2004), with the goal of studying the nature of field OB stars. To date, results include measurement of the field massive star IMF, yielding a power-law slope of  $\Gamma = 2.3 \pm 0.4$ , where the Salpeter value is  $\Gamma = 1.35$  (Lamb et al. 2013); evidence that some OB stars appear to form in the field (Lamb et al. 2010; Oey et al. 2013); discovery of a class of dust-poor B[e] supergiants (Graus et al. 2012); and quantitative parameterization of the field OB population (Lamb et al. 2015).

To identify SMC OB stars, RIOTS4 used two photometric criteria:  $B \leq 15.21$  and  $Q_{UBR} \leq -0.84$ , where  $Q_{UBR}$  is the reddening-free parameter defined as (Oey et al. 2004):

$$Q_{UBR} = (m_U - m_R) - 1.396(m_B - m_R) \quad . \quad (1)$$

In Equation 1,  $m_U$ ,  $m_B$ , and  $m_R$  are the apparent  $U$ ,  $B$ , and  $R$  magnitudes, respectively. These criteria select stars with masses  $\gtrsim 10 M_{\odot}$ . The  $B$  magnitude criterion selects the most luminous stars, while the  $Q_{UBR}$  parameter identifies the bluest stars, corresponding to spectral types of B0 V or B0.5 I and earlier (e.g., Oey et al. 2004). As shown in Equation 1,  $Q_{UBR}$  depends on the  $R$ -band magnitude, which is sensitive to  $H\alpha$ . The Balmer emission that characterizes Oe/Be stars therefore enhances the  $Q_{UBR}$  criterion, promoting completeness of our Oe star sample.

RIOTS4 identified field stars using a friends-of-friends algorithm (Battinelli 1991), which defines field OB stars as stars located farther than a projected distance of 28 pc from any other OB candidate. Thus, the RIOTS4 OB and Oe/Be stars represent a spatially complete sample of all field OB stars that meet the photometric selection criteria.

The RIOTS4 spectroscopic observations were taken using the Magellan Telescopes at Las Campanas Observatory from 2006 to 2011 (Lamb et al. 2015). Details about the observations and data reduction are described by Lamb et al. (2015), so here we present a summary. The majority of spectra were taken using the IMACS spectrograph (Bigelow & Dressler 2003) in its multi-slit mode with a spectral resolution of  $R \sim 2600$  or 3700. A few additional observations were taken using the MIKE echelle spectrograph ( $R \sim 28000$ ) (Bernstein et al. 2003). All RIOTS4 spectra cover the wavelength range 4000–4700 Å; however, the majority extend to  $\sim 5000$  Å, al-

lowing us to identify Oe/Be stars using  $H\beta$ , in addition to  $H\gamma$  and  $H\delta$  emission.

The IMACS multi-slit spectra were reduced using the COSMOS<sup>6</sup> data reduction software, and the 1D spectra were extracted using IRAF<sup>7</sup>. The MIKE and IMACS long-slit spectra were reduced and extracted using IRAF (Lamb et al. 2015). All reductions include background sky subtraction, and none of our Oe star spectra show evidence of any significant contamination from nebular line emission. We also rectified each spectrum and removed cosmic rays. In addition, for 13 low signal-to-noise Oe star spectra, we used the IRAF task `bwfilter` to apply a Fourier filter and remove high-frequency noise. We selected a filter frequency that preserves the double-peaked Balmer emission lines.

### 3. SPECTRAL CLASSIFICATION

We determine the spectral classifications of RIOTS4 O and Oe stars using the photospheric criteria of Walborn and coworkers. For mid O-type stars, the principal diagnostic is the He II  $\lambda 4542$ / He I  $\lambda 4471$  ratio, which is  $\sim 1$  for O7 stars (e.g., Walborn & Fitzpatrick 1990). For late O-types, we use the He II  $\lambda 4200$ / He I  $\lambda 4144$  and He II  $\lambda 4542$ / He I  $\lambda 4387$  ratios, which are  $\sim 1$  for O9 stars (e.g., Sota et al. 2011). The former also distinguishes O9–9.5 stars from B0 stars, since the equivalent width of He II  $\lambda 4200$  decreases for later-type O stars and is  $\sim 0$  for B0 stars (Walborn & Fitzpatrick 1990). In addition, the diagnostics for later O stars act as secondary indicators for early O and Oe stars because the He I  $\lambda 4144$  and He I  $\lambda 4387$  absorption lines do not appear in stars with spectral types earlier than O6–6.5 (e.g., Walborn & Fitzpatrick 1990). Si IV  $\lambda\lambda 4089, 4116$ , Si III  $\lambda 4552$ , and C III  $\lambda 4650$  are also standard diagnostics for late O and early-type B stars; however, these lines are often absent due to the low SMC metallicity. We use them when available, but our classifications necessarily rely on He I and He II lines.

The lack of metal lines also causes problems in determining luminosity classes. The principal diagnostics are N III  $\lambda\lambda 4634-4640-4642$ , He II  $\lambda 4686$ , and the Si IV  $\lambda 4089$ / He I  $\lambda 4026$  ratio (Walborn & Fitzpatrick 1990). Thus, we also use extinction-corrected  $V$  magnitudes from Massey (2002) as an additional criterion, as well as line widths, especially for supergiants.

We also include spectral type modifiers to further characterize our Oe stars. Following the Be star classification system from Lesh (1968), we specify Oe stars whose spectra contain Fe II emission as Oe<sub>+</sub> stars and we use the full Lesh (1968) classification system, e<sub>1</sub> to e<sub>4</sub>, based on Balmer emission line strength. Following Sota et al. (2011), we classify stars whose spectra show He I infill or emission above the continuum as Ope stars, although we follow Negueruela et al. (2004) in using non-infilled He I diagnostics to determine the spectral types of Ope stars. For stars where the equivalent width of He II  $\lambda 4686$  is clearly greater than the equivalent width of He I  $\lambda 4471$

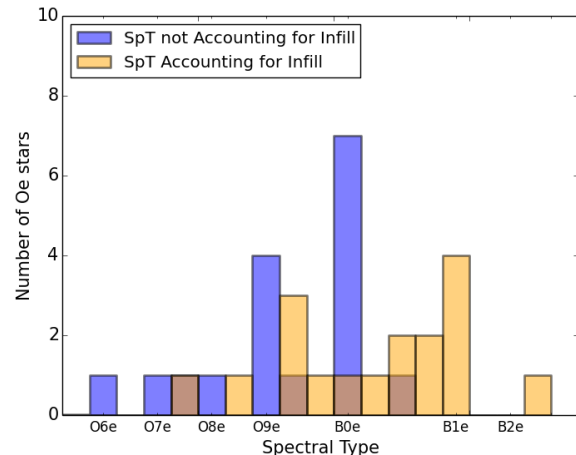


FIG. 1.— Distributions of the spectral types of Oe/Be stars from Negueruela et al. (2004). The blue distribution represents the spectral types from the literature, which are based on the He II  $\lambda 4542$ / He I  $\lambda 4471$  ratio, while the orange distribution represents the Negueruela et al. (2004) classifications obtained without using He I  $\lambda 4471$ .

and He II  $\lambda 4542$ , we add the  $z$  qualifier (Walborn & Blades 1997). Following the usual convention, “:” connotes substantial uncertainty in the classification.

The primary challenge when classifying our Oe stars comes from infill in the He I  $\lambda 4471$  absorption line by disk emission (Steele et al. 1999). Negueruela et al. (2004) find that infill of He I implies that many Oe stars are cooler than their prior classifications suggest. Thus, they reclassified the majority of their Galactic Oe stars as O9.5e or later. Figure 1 highlights this effect by comparing the spectral types presented in Negueruela et al. (2004), determined without using He I  $\lambda 4471$ , to prior classifications from literature of the same stars based on the He II  $\lambda 4542$ / He I  $\lambda 4471$  ratio. Given the importance of infill, we follow Negueruela et al. (2004) and classify our Ope stars without using criteria based on He I  $\lambda 4471$ . Since we cannot rely on metal-line diagnostics, we rely on the He II  $\lambda 4200$ / He I  $\lambda 4144$  and He II  $\lambda 4542$ / He I  $\lambda 4387$  ratios to determine their spectral types. In such cases, we add a “:” to our classification to connote that different classification criteria lead to different spectral types.

At least three of the authors (JBGM, MSO, & JBL) independently classified each RIOTS4 O and Oe star. We compared our results, along with prior ones from literature, to converge on our final classifications for each star, which are accurate to within half a spectral type. About 75% of our classifications agree with values from the literature when available. Table 1 presents the ID’s from Massey (2002) in column 1, and our spectral types in column 2. Columns 3 and 4 provide existing spectral types from the literature and their sources, respectively. The  $V$ -band magnitude (Massey 2002) is given in column 5, extinction  $A_V$  (Zaritsky et al. 2002) in column 6,  $J$ -band magnitude (Skrutskie et al. 2006) in column 7, and  $3.6\mu\text{m}$  magnitude (Gordon et al. 2011) in column 8. Our spectral types for all normal O stars are presented by Lamb et al. (2015). In total, we identify 28–30 Oe stars in RIOTS4; the spectra are presented in the Appendix. Only those with Massey (2002) ID numbers 51373 (Massey et al. 1995), 72535 (Azzopardi et al. 1975), and 75689

<sup>6</sup> COSMOS was written by A. Oemler, K. Clardy, D. Kelson, G. Walsh, and E. Villanueva. See <http://code.obs.carnegiescience.edu/cosmos>.

<sup>7</sup> IRAF is distributed by the National Optical Astronomy Observatory, which is operated by the Association of Universities for Research in Astronomy (AURA), Inc. under cooperative agreement with the National Science Foundation (NSF)

(Evans et al. 2004) have been previously identified as Oe stars.

Star 72535 was classified as O9 Ie by Azzopardi et al. (1975), and we obtain a spectral type of O8–9 I–IIIe. This star has a high luminosity and is brighter in the  $V$  and  $J$ -bands than any other RIOTS4 Oe star (Table 1). As noted, supergiants are not considered classical Oe/Be stars. Star 72535 also shows a high degree of variability for an Oe/Be star (e.g., de Wit et al. 2006; Rivinius et al. 2013), at least 0.4 magnitudes in the 3.6, 4.5, and 5.4  $\mu\text{m}$  bands over only a three month period in 2008, and 0.8 mag in the period from 2005 to 2008 (Gordon et al. 2011). The 2MASS  $J$ -band mag was observed in 1998 (Skrutskie et al. 2006) and not concurrently with the SAGE data, so colors cannot be inferred from these data. Thus, this star does not appear to be a classical Oe star, and we do not include it in our Oe sample in what follows.

#### 4. RESULTS

##### 4.1. The Earliest Oe and Ope Stars

As described in § 1, the decretion disk model predicts that in the low-metallicity SMC, earlier-type Oe stars can form than in the Galaxy, and RIOTS4 reveals some of the earliest known Oe stars to date. Our four earliest have the classifications O6 V((f))e<sub>2</sub>, O6 III((f))e<sub>1</sub>, O6.5 III((f))e<sub>2</sub>, and O7 III(f)e<sub>1</sub> (Figure 2) and Massey (2002) ID numbers 14324, 15271, 69460, and 52363, respectively. These are the earliest unambiguous Oe star classifications reported in the SMC to date. Of these, star 14324 appears to be a shell star, based on its Balmer absorption core. As described in § 3, Oe stars are susceptible to He I infill, especially He I  $\lambda 4471$  (Steele et al. 1999). Thus, many mid and early-type Oe stars that exhibit infill are cooler than suggested by the spectral types obtained using the He II  $\lambda 4542$ / He I  $\lambda 4471$  ratio (Figure 1). In the classification scheme of Sota et al. (2011), such stars should be classified as Ope, but this has not been standardized, and infill can be overlooked. Of particular interest, the MW Oe star HD 39680 has been classified as both O6 V:[n]pe (Sota et al. 2011) and O8.5 Ve (Negueruela et al. 2004); the former corresponds to its spectral type based on the primary diagnostic affected by infill, while the latter is based on secondary diagnostics unaffected by He I infill. The earliest known Oe star in the Galaxy with no evidence of infill appears to be HD 155806, an O7.5 IIIe star (Negueruela et al. 2004). To date, the earliest reported Oe star is Sk – 67 274 (Conti et al. 1986) in the LMC, classified as an O3e star. No published spectrum of this star is available, so we are unable to evaluate whether this is an Ope star. We stress that our four O6e – O7e stars are certainly among the earliest known Oe stars that do *not* show evidence of He I infill.

In Figure 3, we present two Ope stars whose effective temperatures  $T_{\text{eff}}$  may be hotter than that of an O7.5e star. Our spectral types are necessarily uncertain due to He I  $\lambda 4471$  infill, and we base our classifications on the He II  $\lambda 4200$ / He I  $\lambda 4144$  and He II  $\lambda 4542$ / He I  $\lambda 4387$  ratios. The first star, 38036, contains He I  $\lambda 4471$  and  $\lambda 4713$  infill, so we use the He II  $\lambda 4200$ / He I  $\lambda 4144$  and He II  $\lambda 4542$ / He I  $\lambda 4387$  ratios to classify this star. The absence of He I  $\lambda 4144$  and presence of He I  $\lambda 4387$  imply a spectral type of O6.5–7: Vpe<sub>3</sub>. The low signal-to-noise of

the second star, 53360, may allow for infilled He I  $\lambda 4471$  and  $\lambda 4387$ . Thus, we use the He II  $\lambda 4200$ / He I  $\lambda 4144$  ratio to estimate that star 53360 is an O7–9 Vp:e<sub>2</sub> star.

Figure 4 shows three additional early to mid-type Ope stars, which have stronger He I emission than other Ope stars. In particular, all have He I  $\lambda 4713$  and  $\lambda 4471$  in emission. Furthermore, these stars show evidence of infill in the majority of He I lines. Star 59319 shows essentially no He I absorption, and based on the equivalent widths of He II  $\lambda 4200$  and  $\lambda 4542$ , this is an early Ope<sub>3</sub> star, likely earlier than O7.5e. Star 27884 could be as late as O8.5: Vpe<sub>4+</sub>, based on the He I+II  $\lambda 4026$ / He I  $\lambda 4009$  ratio; the absence of C III  $\lambda 4650$  sets our earliest estimate for the spectral type, O7: Vpe<sub>4+</sub>. In addition, we observe Fe II  $\lambda\lambda$  4233, 4583 clearly in emission. The spectrum of 27884 represents the composite of ten observations obtained over four years for binary monitoring, and radial velocity variations suggest that this star may indeed be a binary (see Lamb et al. 2015).

##### 4.1.1. Star 77616: He II $\lambda 4686$ Disk Emission

The third star in Figure 4, 77616 (Azzopardi & Vignneau 1982, AzV 493;), may be the most extreme early Oe/Ope star. The spectrum shows strong He I  $\lambda 4387$ ,  $\lambda 4471$ , and  $\lambda 4713$  emission, and is remarkable because it is the only Oe star with He II  $\lambda 4686$  emission from the Be phenomenon. He II  $\lambda 4686$  emission is associated with stellar winds in Of stars, but the double-peaked line profile here is clearly associated with the circumstellar disk. Furthermore, we do not observe the characteristic N III  $\lambda\lambda 4634$ –40–42 emission of Of stars. Double-peaked He II emission is also associated with Onfp stars, which, as described in § 1, have been proposed as high-mass analogs of the Be phenomenon (Conti & Leep 1974). However, Onfp spectra show Balmer emission only in H $\alpha$ , whereas the spectrum of star 77616 has strong He I infill/emission. Since star 77616 apparently represents the extreme Oe/Be phenomenon at the earliest types, and shows spectral properties that differ strongly from Onfp stars, this further confirms that Oe stars, and not Onfp stars, are the high-mass analogs of the Be phenomenon. He II  $\lambda 4686$  emission is also observed in the spectrum of MWC 656, the Be-black hole X-ray binary (Casares et al. 2014). In MWC 656, He II emission is associated with the accretion disk surrounding the black hole. No X-ray source is identified at the location of star 77616 in the XMM survey of the SMC (Haberl et al. 2012), so it is unlikely that a similar origin can explain the He II emission in 77616. Additionally, there is no discrepancy between the radial velocity of the He II  $\lambda 4686$  emission and the other emission lines.

The He I and He II infill/emission in Ope stars result from  $T_{\text{eff}}$  high enough to singly or doubly photoionize He in the disks. In the case of star 77616, He II emission suggests an extremely high  $T_{\text{eff}}$ . Estimates for ionizing sources of nebular He II  $\lambda 4686$  emission require  $T_{\text{eff}} \geq 60,000$  K (e.g., Garnett et al. 1991), which is extremely rare for main sequence stars. However, models by Brott et al. (2011) suggest that some rapidly-rotating, chemically-homogeneous stars reach this temperature. Oe stars are hot, rapidly rotating massive stars, so they offer an important test of the Brott et al. (2011) models. These models predict that at the SMC metallicity, stars with masses  $\geq 30 M_{\odot}$  and initial rotation veloci-

TABLE 1  
RIOTS4 Oe STARS

ID <sup>a</sup>	SpT <sup>b</sup> (this paper)	SpT (literature)	SpT Source <sup>c</sup>	$V^a$ (mag)	$A_V^d$ (mag)	$J^e$ (mag)	$3.6\mu\text{m}^f$ (mag)
7254	O9.5 IIIe <sub>2</sub>	...	...	14.74	0.86	14.565	13.937
11677	O9 III:e <sub>3+</sub>	...	...	14.46	1.04	14.421	13.655
12102	O9 IIIe <sub>2</sub>	O9.5 V	E04	14.69	0.84	15.113	14.332
14324	O6 V((f))e <sub>2</sub>	...	...	14.11	1.12	13.719	13.031
15271	O6 III((f))e <sub>1</sub>	O6 III((f))	E04	13.54	0.39	13.999	14.105
18329	O9.5 IIIe <sub>4+</sub> pec	...	...	14.65	1.26	14.454	13.630
22321	O9.5 IIIpe <sub>4+</sub>	...	...	13.69	1.00	13.498	12.544
23710	O9-B0 pe <sub>3+</sub>	...	...	14.74	1.31	14.334	13.503
24914	O9 III-Ve <sub>1</sub>	O2((f))+OBe	A09	14.19	0.95	13.682	13.011
27884	O7-8.5 Vpe <sub>4+</sub>	...	...	14.35	1.05	14.275	13.588
30744	O9.5 Ve <sub>2</sub> + B1 III	B0.5 IVe	E04	14.30	0.66	14.563	14.140
37502	O9.5-B0: pe <sub>3+</sub>	...	...	14.62	1.10	14.512	13.723
38036	O6.5-7: Vpe <sub>3</sub>	B0 III	M07	14.33	0.82	14.342	13.884
50095	O9 Ve <sub>4+</sub>	...	...	14.51	0.87	14.440	13.618
51373	O8 IIIze <sub>3</sub>	O7 Ve	M95	13.79	0.84	13.685	13.531
52363	O7 III((f))e <sub>1</sub>	O7 If	E04	14.98	0.38	15.576	15.771
52410	O8 III: ze <sub>3</sub> pec	O8 V	M95	13.75	0.85	13.978	13.298
53360	O7-9 Vp:e <sub>2</sub>	O6-9	E04	15.09	0.77	15.187	14.427
56503	O9 Ve <sub>2</sub>	O9 III-V	E04	14.95	0.68	15.363	14.432
59319	early Ope <sub>3</sub>	...	...	14.32	0.68	14.322	13.435
62638	O9.5 III-Ve <sub>2</sub>	B0 IV	E04	14.67	0.65	14.696	14.562
65318	O9 Ve <sub>1</sub>	...	...	14.95	0.35	15.147	14.918
67673	O9.5 V:e <sub>2</sub>	...	...	14.84	0.83	...	14.974
69460	O6.5 III((f))e <sub>2</sub>	O6.5 If	E04	14.95	0.53	15.121	14.345
72535	O8-9 I-IIIe <sup>g</sup>	O9 Ie	A75	13.45	1.00	13.323	14.031
73795	mid Oe <sub>3+</sub>	O6-9 III-V	E04	14.73	0.82	14.492	13.650
75689	Ope <sub>3</sub> <sup>h</sup>	O4-7 Ve	E04	14.34	0.94	14.174	13.319
75919	O9 IIIe <sub>1</sub>	...	...	14.39	0.78	14.441	14.209
77616	early Ope <sub>3</sub> pec	B0	A82	14.08	1.22	13.959	13.725
78694	O8.5 IIIe <sub>2+</sub>	O9.5 III-V	E04	14.35	0.72	14.342	13.635
82489	O9: IIIpe <sub>4+</sub>	...	...	14.22	0.86	14.195	13.345

<sup>a</sup> Massey (2002)

<sup>b</sup> The subscripts in our spectral classifications are the Lesh (1968) classifications of the Be phenomenon based on the strength of Balmer emission and the presence of Fe II emission.

<sup>c</sup> A09: Antoniou et al. (2009), A75: Azzopardi et al. (1975), A82: Azzopardi & Vigneau (1982), E04: Evans et al. (2004), M07: Martayan et al. (2007b), M95: Massey et al. (1995)

<sup>d</sup> Zaritsky et al. (2002)

<sup>e</sup> Skrutskie et al. (2006)

<sup>f</sup> Gordon et al. (2011)

<sup>g</sup> Not a classical Oe star (see text)

<sup>h</sup> Probably a spectroscopic binary.

ties  $> 400$  km/s reach  $T_{\text{eff}} \sim 60,000$  K at some point in their evolution. The existence of star 77616 is therefore an exciting discovery supporting these predictions. Extremely hot O stars in low-metallicity environments have been proposed as ionizing sources for the He II emission in H II regions that is occasionally observed, especially in extreme starburst galaxies (Kudritzki 2002). Thus, the earliest Oe/Ope stars, like star 77616, may be responsible for this emission.

#### 4.1.2. Ope Stars: Normal Early-Type Oe Stars

As previously discussed, the He I and He II emission that characterize Ope spectra require high temperatures; however, Table 2 shows that strong disk emission is also necessary. The distribution of Lesh (1968) classifications and spectral types in Table 2 shows that nine of ten Ope stars, including star 75689, are Oe<sub>3</sub> or Oe<sub>4</sub> stars, which have the strongest Balmer emission, and thus the strongest disk emission. The only Ope<sub>1</sub> – Ope<sub>2</sub> star has uncertain Ope status: star 53360 has ambiguous He I infill and may not be an Ope star (Figure 3). In total, fifteen RIOTS4 Oe stars, including the nine Ope stars, are Oe<sub>3</sub> or Oe<sub>4</sub> stars, and the six remaining Oe stars have spectral types of O7.5e or later. Furthermore, our earliest

ordinary Oe stars have Lesh (1968) classifications of Oe<sub>1</sub> or Oe<sub>2</sub>, which supports the scenario that the photosphere is visible in early-type Oe stars only if the disk emission is weak. This may be due to high angle of inclination, or physically smaller disks. We do note a tendency for Oe<sub>1</sub> and Oe<sub>2</sub> stars to show double peaked Balmer emission (Figure 8), indicative of high inclinations. Table 2 illustrates that among RIOTS4 Oe<sub>3</sub> and Oe<sub>4</sub> stars, only Ope stars are observed at early spectral types. Therefore, depending on disk emission, it appears that classical Oe stars transition to Ope stars at early spectral types, in particular around type O7e and earlier.

#### 4.1.3. Fe II Emission in Oe Stars

In addition to He I emission, many Oe stars display Fe II emission lines in their spectra. The most common emission lines are Fe II  $\lambda\lambda 4233$ , 4583, and 4629. Similar to the trends with He I emission shown in Table 2, Table 3 shows that Fe II emission also correlates with Lesh (1968) classification and spectral type. All but one Fe II emitting Oe star is a Lesh (1968) Oe<sub>3</sub> or Oe<sub>4</sub> star. We also find that Fe II emission is absent among Oe stars earlier than O7.5e. Interestingly, the frequency of Fe II emission appears to stay constant at approximately 0.50

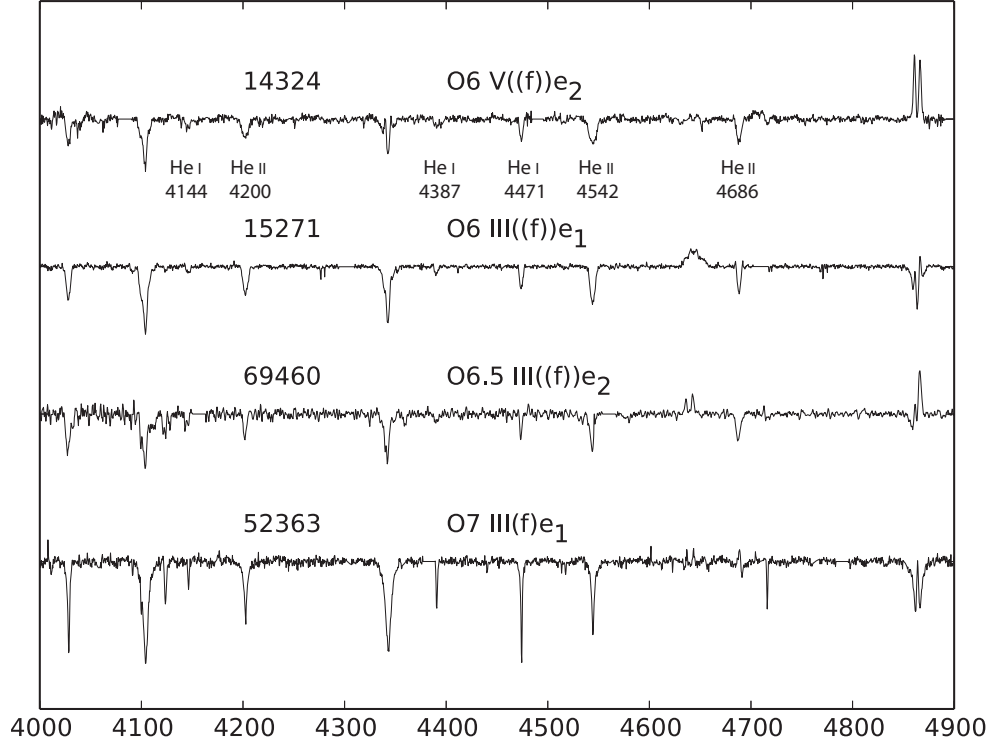


FIG. 2.— The earliest classified RIOTS4 Oe stars. The Massey (2002) ID number and spectral type are listed above each spectrum. The spectral sequence shows that the He II  $\lambda 4542$ / He I  $\lambda 4471$  ratio decreases from earlier to later-type O stars, approaching  $\sim 1$  at O7 (Walborn & Fitzpatrick 1990). The absorption lines used in our classification are also labeled.

TABLE 2  
FREQUENCY OF Ope STARS AMONG RIOTS4 Oe STARS<sup>a</sup>

	early–O7e	O7.5e–8.5e	O9e–9.5e
Oe <sub>1,2</sub>	$0.0 \pm 0.0$ (0,4)	$0.50 \pm 0.35$ (1,2)	$0.11 \pm 0.10$ (1,9)
Oe <sub>3,4</sub>	$1.0 \pm 0.0$ (3,3)	$0.25 \pm 0.22$ (1,4)	$0.57 \pm 0.19$ (4,7)
All Oe	$0.43 \pm 0.20$ (3,7)	$0.33 \pm 0.19$ (2,6)	$0.31 \pm 0.12$ (5,16)

<sup>a</sup> The Ope/Oe ratio, where the denominator includes both Oe and Ope stars in each bin. The numbers in parentheses correspond to the numbers of Ope and Oe + Ope stars, respectively. Star 73795 is included in the O7.5e–8.5e category, and star 75689 is excluded from the table.

among all Oe stars later than O7.5e. Using the preliminary classifications of RIOTS4 Be stars (Lamb et al. 2015), we also find the same Fe II emission lines and the same frequency of Fe II emission. Based on the trends in Tables 2 and 3, the decrease in the  $T_{\text{eff}}$  of O stars promotes Fe II emission for stars strong emission.

#### 4.2. Spectral Type Distribution of Oe Stars

We present the spectral type distribution of RIOTS4 Oe stars in Figure 5. Since  $\sim 20\%$  of our Oe stars have uncertain classifications, we present two distributions, based on the earliest (30 stars; blue) and latest (28 stars; orange) possible spectral type estimates for the uncertain classifications. The number of stars in these distributions differ because the latest possible spectral type for some stars fall into the Be range, which is not included in Fig-

ure 5. Additionally, Figure 5 does not include the two Ope stars and two Oe stars that we are unable to classify.

Figure 5 shows that 53–54% of RIOTS4 Oe stars have spectral types of O9–9.5e. Additionally, stars earlier than O7.5e, including the early Ope stars, account for 21–27% of our sample, unlike in the MW where, to date, no Oe stars in this range have been observed (e.g., Negueruela et al. 2004; Sota et al. 2011, 2014a,b). For the same spectral type distribution as the SMC, we would expect that  $2 \pm 1$  of the eight MW Oe stars should have spectral types earlier than O7.5e. Thus, our results demonstrate that, compared to the MW, the distribution of Oe stars in the SMC field is significantly enhanced towards earlier-type stars. We caution that McBride et al. (2008) find that the spectral type distributions of Be/X-ray binaries in the SMC and MW are similar, whereas Negueruela



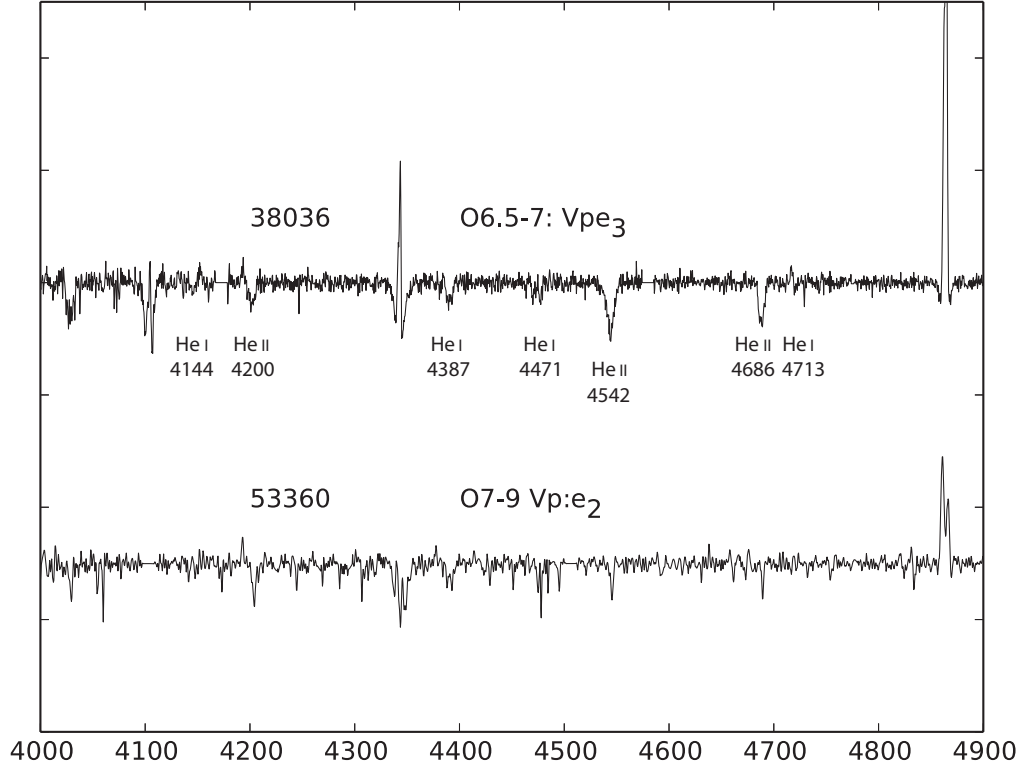


FIG. 3.— Spectra of the RIOTS4 Ope stars that may be hotter than O7.5e stars; both show infill in He I  $\lambda 4471$ . The Massey (2002) ID number and spectral type appear above each spectrum. The absorption lines used to classify these stars and the He I lines in infill/emission are also labeled.

TABLE 3  
FREQUENCY OF Fe II EMISSION AMONG RIOTS4 Ope STARS<sup>a</sup>

	early-O7e	O7.5e–8.5e	O9e–9.5e
Oe <sub>1,2</sub>	$0.0 \pm 0.0$ (0,4)	$0.50 \pm 0.35$ (1,2)	$0.0 \pm 0.0$ (0,9)
Oe <sub>3,4</sub>	$0.0 \pm 0.0$ (0,3)	$0.50 \pm 0.25$ (2,4)	$1.0 \pm 0.0$ (7,7)
All Oe	$0.0 \pm 0.0$ (0,7)	$0.50 \pm 0.20$ (3,6)	$0.44 \pm 0.12$ (7,16)

<sup>a</sup> The frequency of Oe stars with Fe II emission, where the denominator includes the total number of Oe stars in each bin. The numbers in parentheses are the number of Oe stars with Fe II emission and the total number of Oe stars. As before, star 73795 is included in the O7.5e–8.5e category, and star 75689 is excluded from the table.

(1998) finds quite different distributions between Be stars and Be/X-ray binaries in the MW.

We calculate the Oe/O ratio using the 28–30 Oe stars we identify and the 106–109 RIOTS4 O stars (Lamb et al. 2015), which include Oe stars and exclude supergiants. As noted, ambiguity in the spectral types of stars whose classifications allow them to fall into the early B-star range causes the uncertainty. Table 4 shows the Oe/O ratios and binomial errors at each spectral type. Columns 2 and 3 show the values based on the earliest and latest possible spectral types for stars with uncertain classifications. We find that the frequency of Oe stars is approximately constant between  $\sim 0.15 - 0.30$  with a possible increase at the earliest spectral types, although we

caution that stochastic effects are worst for the earliest bin.

#### 4.3. Metallicity and the Frequency of Oe stars

We measure an Oe/O ratio of  $0.26 \pm 0.04$  ( $0.27 \pm 0.04$ ) when considering the latest (earliest) possible spectral types for RIOTS4. We adopt the value from the latest spectral types, in what follows. We compare our Oe star frequency to an estimate by Bonanos et al. (2010) based on photometric identifications of a sample of 208 previously classified O stars, in which Oe star candidates are identified using IR photometry from the the IR Survey Facility (IRSF) Magellanic Clouds Point Source Catalog (Kato et al. 2007) and *Spitzer* SAGE-SMC survey (Gor-



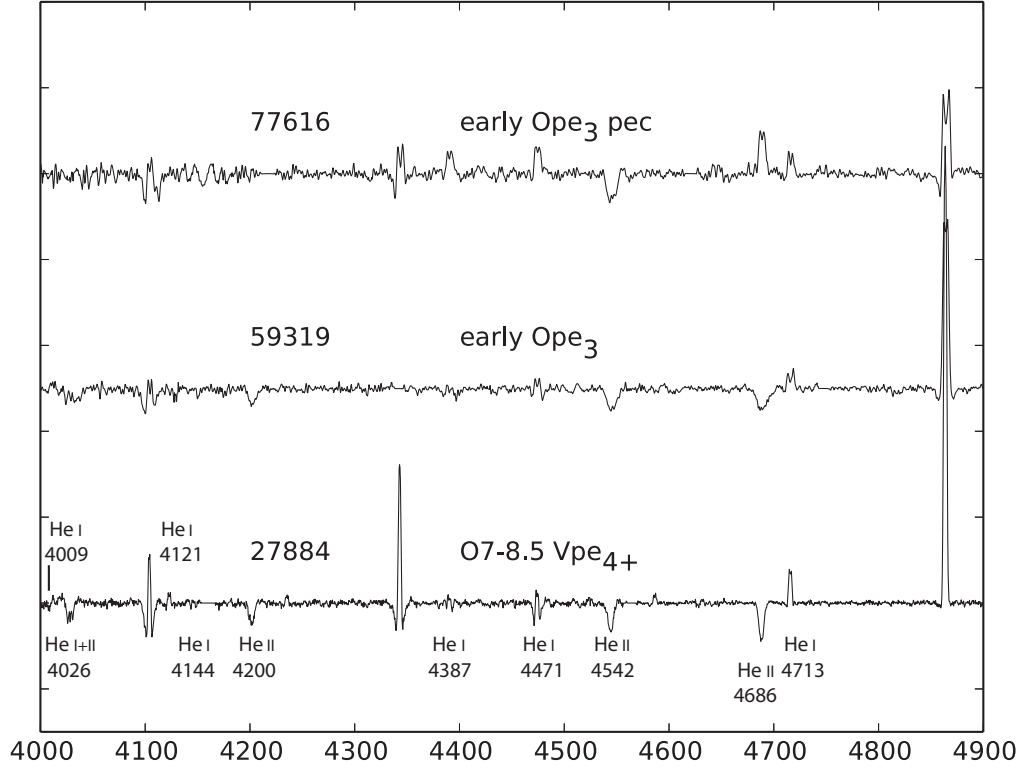


FIG. 4.— The three extreme early-type RIOTS4 Ope stars, all with He I  $\lambda 4713$  in emission. The Massey (2002) ID number and spectral type appear above each spectrum. The He I and He II features in infill and emission are also labeled.

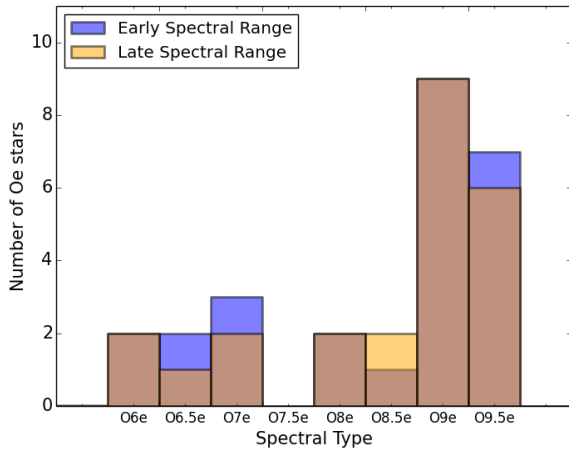


FIG. 5.— The number of Oe stars observed at each spectral type. To account for uncertainty in the spectral types of  $\sim 20\%$  of our stars, the two distributions represent those obtained using our earliest estimate (blue) and latest (orange) for stars with uncertain spectral types. Stars without spectral types are not included in this figure.

don et al. 2011). Although the stars have existing spectral types, Bonanos et al. (2010) use NIR photometry to more consistently identify Oe star candidates in their heterogeneous sample. They obtain an Oe/O ratio of  $0.10 \pm 0.02$  using the selection criteria  $J_{\text{IRSF}} - [3.6] > 0.5$

TABLE 4  
Oe/O RATIO AT EACH SPECTRAL TYPE<sup>a</sup>

SpT	Oe/O Earliest	Oe/O Latest
O6–6.5	$0.57 \pm 0.19$ (4)	$0.50 \pm 0.20$ (3)
O7–7.5	$0.21 \pm 0.11$ (3)	$0.17 \pm 0.11$ (2)
O8–8.5	$0.11 \pm 0.06$ (3)	$0.14 \pm 0.07$ (4)
O9–9.5	$0.30 \pm 0.06$ (16)	$0.29 \pm 0.06$ (15)

<sup>a</sup> The number of Oe stars in each spectral type range is listed in parentheses. The stars we are unable to classify are not included.

and  $J_{\text{IRSF}} < 15$ .

We find that 12 of the 16 Oe star candidates Bonanos et al. (2010) identified were spectroscopically observed in H $\alpha$  and show emission (Evans et al. 2004; Meyssonnier & Azzopardi 1993), although one is a supergiant, which cannot be a classical Oe/Be star. We confirm that two H $\alpha$ -emitters are RIOTS4 Oe stars and one we classify as a Be star. Of the four remaining candidates, one is a RIOTS4 Oe star, two show no Balmer emission in existing spectra from the literature, and one shows only nebular emission (Evans et al. 2004). Thus, 75% of the Bonanos et al. (2010) candidates are likely Oe stars, a reasonably good return.

However, the Bonanos et al. (2010) color criterion, based on the  $J - [3.6]$  colors of four previously identi-

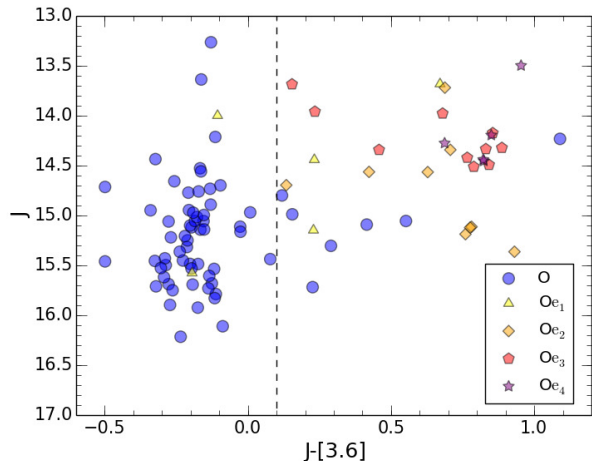


FIG. 6.— IR color-magnitude diagram for RIOTS4 O and Oe stars. The key shows symbols for normal O stars and Oe stars, divided by their Lesh (1968) classifications. The vertical dashed line shows our revised Oe star candidate photometric criterion,  $J - [3.6] \geq 0.1$ . We caution that the  $J$  and  $[3.6]$  data were observed many years apart, so the colors have significant uncertainty due to possible variability (see text).

fied SMC Oe stars, causes the discrepancy between their Oe/O ratio and ours. Figure 6 shows the  $J$  vs  $J - [3.6]$  color-magnitude diagram for RIOTS4 O and Oe stars, using  $J$ -band magnitudes from the Two-Micron All Sky Survey (2MASS; Skrutskie et al. 2006), and  $3.6\mu\text{m}$ -band magnitudes from the *Spitzer* SAGE-SMC survey (Gordon et al. 2011) (Table 1). One Oe and ten O stars are omitted from Figure 6 because the IR magnitudes are unavailable. Figure 6 shows that the Bonanos et al. (2010) criteria exclude 13 of our  $28 \pm 1$  spectroscopically identified Oe stars with IR data. We therefore propose a revised criterion,  $J - [3.6] \geq 0.1$ , to select Oe candidates, which accounts for all but two RIOTS4 Oe<sub>1</sub> stars, both of which have infilled Balmer lines, corresponding to the weakest presentation of the Oe/Be phenomenon (Lesh 1968).

Applying our  $J - [3.6]$  criterion to the Bonanos et al. (2010) sample increases the number of their Oe star candidates from 16 to 34, and raises their Oe star frequency to  $0.22 \pm 0.03$ . Similarly, applying our color criterion to RIOTS4, we identify 7 new RIOTS4 Oe star candidates. These may or may not be Oe stars; their RIOTS4 spectra show no  $H\beta$ ,  $H\gamma$  or  $H\delta$  emission, but they may have  $H\alpha$  emission, which is beyond our observed spectral range. Additionally, the strength of the Be phenomenon may have varied between when the *Spitzer* SAGE-SMC and RIOTS4 observations were taken. In any case, including all 7 candidates raises our Oe/O ratio to  $0.35 \pm 0.05$  from our spectroscopic value,  $0.26 \pm 0.04$ . We note that our formal uncertainties still show agreement between our photometric selection and spectroscopic identifications. There are a few stars in Figure 6 whose classifications are inconsistent with the colors according to our criterion, and these may have incorrect  $J - [3.6]$  colors if the magnitudes varied between the two photometric observations. The 2MASS  $J$ -band observations were obtained between 1997–2001 (Skrutskie et al. 2006), while the the SAGE  $3.6\mu\text{m}$  data were observed in 2005 and 2008 (Gordon et al. 2011). We note that our classical Oe

stars do not show significant variability in their  $3.6\mu\text{m}$  magnitudes. The modest discrepancy between our photometrically determined frequency and the revised Bonanos et al. (2010) value may be caused by such color errors and differences in sample selection. RIOTS4 is a complete sample of SMC field O stars, while the Bonanos et al. (2010) sample is heterogeneous, selecting all O stars with existing spectral classifications.

Figure 6 shows that O stars have  $J - [3.6] \sim -0.2$ , as expected from the Rayleigh-Jeans portion of an O star blackbody curve, whereas Oe stars are clustered near  $J - [3.6] \sim 0.8$ . Additionally, the  $J - [3.6]$  colors of our Oe stars match those of spectroscopically confirmed SMC Be stars from Figure 10 of Bonanos et al. (2010). The only difference between Oe and Be stars in these bands is that Be stars have  $J$  magnitudes between 14 and 18, while Oe stars have  $J \sim 13$  to 15, highlighting that Oe stars are the more luminous extension of the Be phenomenon. In Figure 6, it is especially interesting that stars concentrated in the clump at  $J - [3.6] \sim 0.8$  have the highest-value Lesh (1968) classifications, Oe<sub>3</sub> and Oe<sub>4</sub>, corresponding to the strongest Be phenomena. Thus, these stars must have the largest disks. The range in  $J - [3.6]$  values presumably results from disks of different sizes, which may correspond to different growth stages. Disk viewing angle also plays an important role.

Figure 6 also shows that Oe stars are on average approximately 1 magnitude brighter than O stars in the  $J$ -band, where the flux from the circumstellar disk strongly dominates over that from the stellar photosphere. The excess flux has been observed to reach up to half a magnitude in the visible bands and dominates in the IR (e.g., Rivinius et al. 2013). We created a simple model of the combined blackbody emission of an SMC O9.5 star with  $T_{\text{eff}} \sim 31,000$  K and  $\log g \sim 4.2$  (Georgy et al. 2013) and a disk with emission approximated using the thin disk model of Adams et al. (1987). Using this model, we reproduce a 1 mag  $J$ -band excess and a 0.2 magnitude  $V$ -band excess when adopting inner and outer radii of  $7R_*$  and  $10R_*$ , respectively, where  $R_*$  is the stellar radius. This is not meant to be a realistic representation of a Be-star disk, but serves to illustrate that the observed thermal emission properties are consistent with reasonable parameters. Additionally, the somewhat evolved nature of Oe/Be stars may enhance their total luminosities.

Using the Bonanos et al. (2010) sample of OB stars, Kournotis et al. (2014) also attempt to identify Oe candidates, using photometric light curves from OGLE III (Udalski et al. 2008), a  $VI$  photometric survey of the SMC. Their criteria are based on irregular variability and a color criterion, yielding an Oe/O ratio of  $0.13 \pm 0.02$ . Since they use the same sample as Bonanos et al. (2010), the color criterion suggests that a similar revision may rescale the Kournotis et al. (2014) frequency to a value more consistent with our own.

In the Galaxy, only eight Oe stars are found in the GOSSS survey (Sota et al. 2011, 2014a,b), yielding a frequency of spectroscopically identified Oe stars of  $0.03 \pm 0.01$ , far less than our spectroscopic SMC field measurement,  $0.26 \pm 0.04$ . We caution that the MW estimate may be missing some Oe stars, as mentioned in § 1, and that comparison of the GOSSS and RIOTS4 statistics is problematic due to the different sample selection; GOSSS is a Galactic, magnitude-limited survey,

while RIOTS4 is a spatially complete sample of SMC field OB stars. Given the lack of Oe star samples, the GOSSS estimate is one of the few we can compare to our measurements. Keeping in mind the possible biases, the relative incidence of Oe stars in these two environments strongly supports the decretion disk model. Our results are also similar to the trend reported by Martayan et al. (2010), that the Be phenomenon is enhanced by a factor of 3–5 among earlier-type OB stars in the SMC, compared to the MW.

As mentioned in § 4.1, the LMC O3e star, Sk –67 274 (Conti et al. 1986), may be the earliest-type Oe star currently known. While we did not identify an O3e star in the SMC, this galaxy has fewer stars than the LMC, so the probability of hosting an O3e star is lower. We evaluate the likelihood of observing an O3e star in the LMC by comparing the frequency of Oe and Be stars in the MW, LMC, and SMC. The Be/B ratios are  $0.17 \pm 0.03$  (Zorec & Briot 1997, see § 1),  $0.175 \pm 0.025$  (Martayan et al. 2006b), and  $0.26 \pm 0.04$  (Martayan et al. 2007a) in the fields of these galaxies, respectively. Similarly, we find that the Oe/O ratios are  $0.03 \pm 0.01$  in the MW and  $0.26 \pm 0.04$  in the SMC field. We use the ratios between the Be and Oe star frequencies and the trend with metallicity to estimate a lower limit on the frequency of Oe stars in the LMC of  $\sim 0.06$ . There are approximately two dozen O3 stars in the LMC, excluding the 30 Dor region (Skiff 2014; Walborn et al. 2014). If we assume the frequency of Oe stars is constant across all spectral types, then we expect to find one O3e star in the LMC. Thus, the observed O3e star in the LMC is consistent with the metallicity trend, without considering the status of Ope stars.

#### 4.4. Field vs. Cluster Environment and the Frequency of Oe Stars

Although we find that our SMC field Oe/O ratio is much greater than the estimate for the MW, we again caution that our sample contains only field stars, which may bias a comparison to the GOSSS sample. As described in § 1, on average, Galactic cluster OB stars rotate faster than their counterparts in the field (Guthrie 1984; Wolff et al. 2007, 2008), which should cause the frequency of Oe/Be stars to be higher in clusters. Turning to the SMC, Martayan et al. (2010) measure the frequency of Oe stars in SMC clusters to be  $0.24 \pm 0.09^8$  among O8–9 stars, binned in integer spectral types, which agrees well with our Oe/O ratio of  $0.24 \pm 0.05$  for the same spectral range. We caution that the spectral types from Martayan et al. (2010) are rough estimates based on *BVI* colors and the absolute *V* magnitude. However, the similarity between these frequencies is consistent with measurements for the Be/B ratio in the SMC field and clusters from Martayan et al. (2007a): for SMC clusters and the field surrounding NGC 330, the Be/B ratios are estimated to be 0.20–0.40 and  $0.26 \pm 0.04$  respectively. When examining the average rotational velocities for field and cluster B stars, Martayan et al. (2007b) find no significant difference, obtaining  $159 \pm 20$  km/s and  $163 \pm 18$  km/s, respectively. Thus, unlike in the Galaxy,

in the SMC, B stars do not rotate more slowly in the field than in clusters, which is consistent with the similarity in the frequency of Oe/Be stars in these environments.

## 5. DISCUSSION

The VDD model requires rapid rotation, which stellar winds, and hence high metallicity, inhibit. Trends with rotational velocity should correlate with Oe/Be star frequencies and our sample of field SMC Oe stars strongly supports the qualitative predictions of this model. In the metal-poor SMC, the Oe/Be phenomenon should extend to earlier spectral types, and our data confirm this trend, although we caution that the Galactic distribution of Oe star spectral types is dominated by small number statistics. We find four Oe stars with spectral types earlier than the earliest MW Oe star, and five additional Ope stars which may have temperatures representative of similar, and even earlier, spectral types. We also measure an Oe/O ratio of  $0.26 \pm 0.04$ , which is much greater than the MW value,  $0.03 \pm 0.01$ , and is consistent with the expected anticorrelation with metallicity. Additionally, the pattern in rotation rates between field and cluster environments in the SMC is consistent with the pattern in Oe star frequencies. Thus, our data show three trends consistent with expectations from the decretion disk model, and confirm that Oe stars are the high-mass extension of the Be phenomenon. By the same token, our Oe star frequency offers further evidence against the previously proposed wind-compressed disk and magnetic-compressed disk models for the Be phenomenon, because both models rely on strong stellar winds to form a circumstellar disk (e.g. Bjorkman & Cassinelli 1993; Cassinelli et al. 2002), and therefore predict a correlation with metallicity; this contradicts our observed anti-correlation.

## 6. CONCLUSIONS

We present a complete sample of Oe stars identified from RIOTS4, a spatially complete, spectroscopic survey of SMC field OB stars (Lamb et al. 2015). We find  $29 \pm 1$  Oe stars, of which only two have previously been identified. Ten are Ope stars, which exhibit He I in-fill and/or emission. This complete sample of Oe stars offers an unprecedented opportunity to examine the classical Oe/Be phenomenon in a low-metallicity, field environment. In particular, our conventional understanding of Oe/Be stars is that they host rotationally induced decretion disks, whose formation is suppressed at higher metallicity due to strong stellar winds that strip angular momentum from the stars.

Thus, weaker stellar winds in the low-metallicity SMC should produce earlier-type Oe stars than in the Galaxy, and this is consistent with our observations. Our spectral type distribution (Figure 5) shows that 21–27% of our Oe stars are earlier than O7.5e, the earliest MW Oe star spectral type (Negueruela et al. 2004). We find four Oe stars (Figure 2) that have spectral types in this range: stars 14324 (O6 V((f))e<sub>2</sub>), 15271 (O6 III((f))e<sub>1</sub>), 69460 (O6.5 III((f))e<sub>2</sub>), and 52363 (O7 III(f)e<sub>1</sub>). The O6e stars are the earliest classified Oe stars in the SMC, and possibly the earliest unambiguous, non-Ope classifications of classical Oe stars known to date. Furthermore, we identify five Ope stars (Figures 3 and 4) with  $T_{\text{eff}}$  corresponding to similarly early spectral types. The hottest Ope star, 77616 (Figure 4), shows He II  $\lambda 4686$

<sup>8</sup> Martayan et al. (2010) do not present an uncertainty for this value, so we calculate the binomial error from the data in their paper.

emission, demonstrating that in low-metallicity environments, even the very hottest O stars can presumably form decretion disks.

In addition, the weak stellar winds in the metal-poor SMC should produce a higher frequency of Oe stars than in the higher-metallicity MW. Consistent with this prediction, we measure an Oe/O ratio of  $0.26 \pm 0.04$ , an order of magnitude greater than our MW estimate,  $0.03 \pm 0.01$ . Furthermore, this trend is also seen in Be stars, which are 3–5 times more frequent among early-type stars in the SMC than in the MW (Martayan et al. 2010).

The correlation between rotation velocities and Oe star frequencies also supports the decretion disk model. In the Galaxy, field OB stars rotate more slowly than their cluster counterparts, so we expect the Oe/O ratio to be higher in clusters than in the field. However, in the SMC, no significant difference is observed between field and cluster B star rotation velocities (Martayan et al. 2007b). The Oe/O ratio ( $0.25 \pm 0.05$ ), as measured for O8–9 stars among our SMC field sample, and the corresponding cluster estimate from Martayan et al. (2010) ( $0.24 \pm 0.09$ ) are in agreement. Thus, our data for SMC Oe stars are consistent with predictions for how metallicity, stellar winds, and environment affect decretion disk formation, and confirm that Oe stars are the high-mass extension of the Be phenomenon.

Another fundamental result to emerge from our study is that for mid and early O spectral types, the Oe/Be phenomenon manifests as Ope spectra, exhibiting He I infill/emission. This is seen from Table 2, which illustrates that Ope stars are more common among earlier-type stars. Additionally, our data suggest that Ope stars are associated with Lesh (1968) Oe<sub>3</sub> and Oe<sub>4</sub> classifications and dominate for spectral types earlier than  $\sim$ O7.5e. Furthermore, our earliest ordinary Oe stars are Oe<sub>1</sub> or Oe<sub>2</sub> stars. This indicates that photospheric He I and He II absorption lines are visible when disk emission is weak, corresponding to Lesh (1968) classifications of Oe<sub>1</sub> and Oe<sub>2</sub>. The He I disk emission is thus simply coincident with H Balmer emission in the early types. At

the earliest extreme, we even find He II disk emission. Additionally, Fe II emission is more common among Oe<sub>3</sub> and Oe<sub>4</sub> classifications; approximately 50% of late-Oe and early-Be type stars have Fe II emission.

We also revise a NIR color selection criterion for Oe stars (Bonanos et al. 2010) to  $J - [3.6] \geq 0.1$ , which more accurately recovers our spectroscopically identified Oe stars, especially those with weaker Balmer emission (Figure 6). In addition, we find that Oe stars are systematically brighter than ordinary O stars by about 1 mag in the *J*-band, likely due to either disk emission and/or Oe stars being somewhat evolved.

Finally, our discovery of the extreme Ope star, 77616, which shows the Oe/Be phenomenon in both He I and He II emission, offers observational support for theoretical predictions that the hottest, rapidly rotating, low-metallicity O stars can reach He II-producing  $T_{\text{eff}}$ . The He II Ope emission of star 77616 is consistent with models by Brott et al. (2011) for stars  $\gtrsim 30 M_{\odot}$  with rotation velocities  $> 400$  km/s at SMC metallicity, yielding rotationally mixed stars with  $T_{\text{eff}} \sim 60,000$  K. Since Oe stars are the most rapidly rotating O stars, we suggest that extreme Oe/Ope stars may be responsible for He II emission occasionally seen in H II regions and extreme starburst galaxies. Thus, our results show that even the hottest O stars can present the Oe/Be phenomenon and produce decretion disks.

We thank the referee, Ignacio Negueruela, for useful and insightful feedback. We also thank Jon Bjorkman, Karen Bjorkman, Xiao Che, Peter Conti, Selma de Mink, Jesús Maíz-Apellániz, Philip Massey, Megan Reiter, John Monnier, Thomas Rivinius, and Aaron Sigt for useful discussions. We also thank Ian Roederer for helpful comments on a draft of this paper. Additionally, JBG thanks Daniel Gifford for a variety of help, including with python programming and statistics. This work was supported by NSF grants AST-0907758 and AST-1514838.

## REFERENCES

- Adams, F. C., Lada, C. J., & Shu, F. H. 1987, *ApJ*, 312, 788  
 Antoniou, V., Hatzidimitriou, D., Zezas, A., & Reig, P. 2009, *ApJ*, 707, 1080  
 Azzopardi, M., & Vignneau, J. 1982, *A&AS*, 50, 291  
 Azzopardi, M., Vignneau, J., & Macquet, M. 1975, *A&AS*, 22, 285  
 Battinelli, P. 1991, *A&A*, 244, 69  
 Bernstein, R., Sackett, S. A., Gunnels, S. M., Mochnacki, S., & Athey, A. E. 2003, in *Society of Photo-Optical Instrumentation Engineers (SPIE) Conference Series*, Vol. 4841, *Instrument Design and Performance for Optical/Infrared Ground-based Telescopes*, ed. M. Iye & A. F. M. Moorwood, 1694–1704  
 Bigelow, B. C., & Dressler, A. M. 2003, in *Society of Photo-Optical Instrumentation Engineers (SPIE) Conference Series*, Vol. 4841, *Instrument Design and Performance for Optical/Infrared Ground-based Telescopes*, ed. M. Iye & A. F. M. Moorwood, 1727–1738  
 Bjorkman, J. E., & Cassinelli, J. P. 1993, *ApJ*, 409, 429  
 Bonanos, A. Z., Lennon, D. J., Köhlinger, F., et al. 2010, *AJ*, 140, 416  
 Brott, I., de Mink, S. E., Cantiello, M., et al. 2011, *A&A*, 530, A115  
 Casares, J., Negueruela, I., Ribó, M., et al. 2014, *Nature*, 505, 378  
 Cassinelli, J. P., Brown, J. C., Maheswaran, M., Miller, N. A., & Telfer, D. C. 2002, *ApJ*, 578, 951  
 Chauville, J., Zorec, J., Ballereau, D., et al. 2001, *A&A*, 378, 861  
 Collins, II, G. W. 1987, in *IAU Colloq. 92: Physics of Be Stars*, ed. A. Slettebak & T. P. Snow, 3–19  
 Conti, P. S., Garmany, C. D., & Massey, P. 1986, *AJ*, 92, 48  
 Conti, P. S., & Leep, E. M. 1974, *ApJ*, 193, 113  
 de Mink, S. E., Langer, N., Izzard, R. G., Sana, H., & de Koter, A. 2013, *ApJ*, 764, 166  
 de Wit, W. J., Lamers, H. J. G. L. M., Marquette, J. B., & Beaulieu, J. P. 2006, *A&A*, 456, 1027  
 Diago, P. D., Gutiérrez-Soto, J., Fabregat, J., & Martayan, C. 2009, *Communications in Asteroseismology*, 158, 184  
 Divan, L., Zorec, J., & Andrillat, Y. 1983, *A&A*, 126, L8  
 Ekström, S., Meynet, G., Maeder, A., & Barblan, F. 2008, *A&A*, 478, 467  
 Ekström, S., Georgy, C., Eggenberger, P., et al. 2012, *A&A*, 537, A146  
 Evans, C. J., Howarth, I. D., Irwin, M. J., Burnley, A. W., & Harries, T. J. 2004, *MNRAS*, 353, 601  
 Frémat, Y., Zorec, J., Hubert, A.-M., & Floquet, M. 2005, *A&A*, 440, 305  
 Frost, S. A., & Conti, P. S. 1976, in *IAU Symposium*, Vol. 70, *Be and Shell Stars*, ed. A. Slettebak, 139  
 Garnett, D. R., Kennicutt, Jr., R. C., Chu, Y.-H., & Skillman, E. D. 1991, *PASP*, 103, 850  
 Georgy, C., Ekström, S., Eggenberger, P., et al. 2013, *A&A*, 558, A103

- Gordon, K. D., Meixner, M., Meade, M. R., et al. 2011, *AJ*, 142, 102
- Graus, A. S., Lamb, J. B., & Oey, M. S. 2012, *ApJ*, 759, 10
- Guthrie, B. N. G. 1984, *MNRAS*, 210, 159
- Haberl, F., Sturm, R., Ballet, J., et al. 2012, *A&A*, 545, A128
- Hanuschik, R. W. 1996, *A&A*, 308, 170
- Huang, W., & Gies, D. R. 2008, *ApJ*, 683, 1045
- Huang, W., Gies, D. R., & McSwain, M. V. 2010, *ApJ*, 722, 605
- Kato, D., Nagashima, C., Nagayama, T., et al. 2007, *PASJ*, 59, 615
- Kourniotis, M., Bonanos, A. Z., Soszyński, I., et al. 2014, *A&A*, 562, A125
- Kudritzki, R. P. 2002, *ApJ*, 577, 389
- Lamb, J. B., Oey, M. S., Graus, A. S., Adams, F. C., & Segura-Cox, D. M. 2013, *ApJ*, 763, 101
- Lamb, J. B., Oey, M. S., Segura-Cox, D. M., et al. 2015, *ApJ*, in press
- Lamb, J. B., Oey, M. S., Werk, J. K., & Ingleby, L. D. 2010, *ApJ*, 725, 1886
- Langer, N. 1998, *A&A*, 329, 551
- Lee, U., Osaki, Y., & Saio, H. 1991, *MNRAS*, 250, 432
- Lesh, J. R. 1968, *ApJS*, 17, 371
- Levesque, E. M., Leitherer, C., Ekstrom, S., Meynet, G., & Schaerer, D. 2012, *ApJ*, 751, 67
- Maeder, A., & Meynet, G. 2001, *A&A*, 373, 555
- Maíz-Apellániz, J., Walborn, N. R., Galué, H. Á., & Wei, L. H. 2004, *ApJS*, 151, 103
- Martayan, C., Baade, D., & Fabregat, J. 2010, *A&A*, 509, A11
- Martayan, C., Floquet, M., Hubert, A. M., et al. 2007a, *A&A*, 472, 577
- Martayan, C., Frémat, Y., Hubert, A.-M., et al. 2006a, *A&A*, 452, 273
- . 2007b, *A&A*, 462, 683
- Martayan, C., Hubert, A. M., Floquet, M., et al. 2006b, *A&A*, 445, 931
- Massey, P. 2002, *ApJS*, 141, 81
- Massey, P., Lang, C. C., Degioia-Eastwood, K., & Garmany, C. D. 1995, *ApJ*, 438, 188
- McBride, V. A., Coe, M. J., Negueruela, I., Schurch, M. P. E., & McGowan, K. E. 2008, *MNRAS*, 388, 1198
- McLaughlin, D. B. 1961, *JRASC*, 55, 73
- McSwain, M. V., & Gies, D. R. 2005, *ApJS*, 161, 118
- Meilland, A., Millour, F., Kanaan, S., et al. 2012, *A&A*, 538, A110
- Meynet, G., & Maeder, A. 2003, *A&A*, 404, 975
- Meyssonnier, N., & Azzopardi, M. 1993, *A&AS*, 102, 451
- Negueruela, I. 1998, *A&A*, 338, 505
- Negueruela, I., Steele, I. A., & Bernabeu, G. 2004, *Astronomische Nachrichten*, 325, 749
- Oey, M. S., King, N. L., & Parker, J. W. 2004, *AJ*, 127, 1632
- Oey, M. S., Lamb, J. B., Kushner, C. T., Pellegrini, E. W., & Graus, A. S. 2013, *ApJ*, 768, 66
- Owoc, S. 2006, 355, 219
- Porter, J. M. 1999, *A&A*, 348, 512
- Rauw, G., Naze, Y., Marique, P. X., et al. 2007, *Information Bulletin on Variable Stars*, 5773, 1
- Rivinius, T., Carciofi, A. C., & Martayan, C. 2013, *A&A Rev.*, 21, 69
- Rivinius, T., Štefl, S., & Baade, D. 2006, *A&A*, 459, 137
- Sana, H., Le Bouquin, J.-B., Lacour, S., et al. 2014, *ApJS*, 215, 15
- Skiff, B. A. 2014, *VizieR Online Data Catalog*, 1, 2023
- Skrutskie, M. F., Cutri, R. M., Stiening, R., et al. 2006, *AJ*, 131, 1163
- Sota, A., Maíz Apellániz, J., Morrell, N. I., et al. 2014a, *ApJS*, 211, 10
- Sota, A., Maíz Apellániz, J., Walborn, N. R., et al. 2014b, *VizieR Online Data Catalog*, 3274, 0
- Sota, A., Maíz Apellániz, J., Walborn, N. R., et al. 2011, *ApJS*, 193, 24
- Steele, I. A., Negueruela, I., & Clark, J. S. 1999, *A&AS*, 137, 147
- Stoeckley, T. R. 1968, *MNRAS*, 140, 141
- Struve, O. 1931, *ApJ*, 73, 94
- Townsend, R. H. D., Owoc, S. P., & Howarth, I. D. 2004, *MNRAS*, 350, 189
- Udalski, A., Soszyński, I., Szymański, M. K., et al. 2008, *ActaA*, 58, 329
- Vink, J. S., Davies, B., Harries, T. J., Oudmaijer, R. D., & Walborn, N. R. 2009, *A&A*, 505, 743
- Walborn, N. R. 1973, *AJ*, 78, 1067
- Walborn, N. R., & Blades, J. C. 1997, *ApJS*, 112, 457
- Walborn, N. R., & Fitzpatrick, E. L. 1990, *PASP*, 102, 379
- Walborn, N. R., Howarth, I. D., Evans, C. J., et al. 2010, *AJ*, 139, 1283
- Walborn, N. R., Sana, H., Simón-Díaz, S., et al. 2014, *A&A*, 564, A40
- Wolff, S. C., Strom, S. E., Cunha, K., et al. 2008, *AJ*, 136, 1049
- Wolff, S. C., Strom, S. E., Dror, D., & Venn, K. 2007, *AJ*, 133, 1092
- Zaritsky, D., Harris, J., Thompson, I. B., Grebel, E. K., & Massey, P. 2002, *AJ*, 123, 855
- Zorec, J., & Briot, D. 1997, *A&A*, 318, 443

## APPENDIX

Here we present all of our RIOTS4 Oe and Ope spectra. We organize the stars by spectral type, from earliest to latest. Figures 7 and 8 present luminosity class V stars and luminosity class III stars, respectively. We label the principal absorption lines used for our classification criteria as well as Fe II, He I, and He II emission lines.

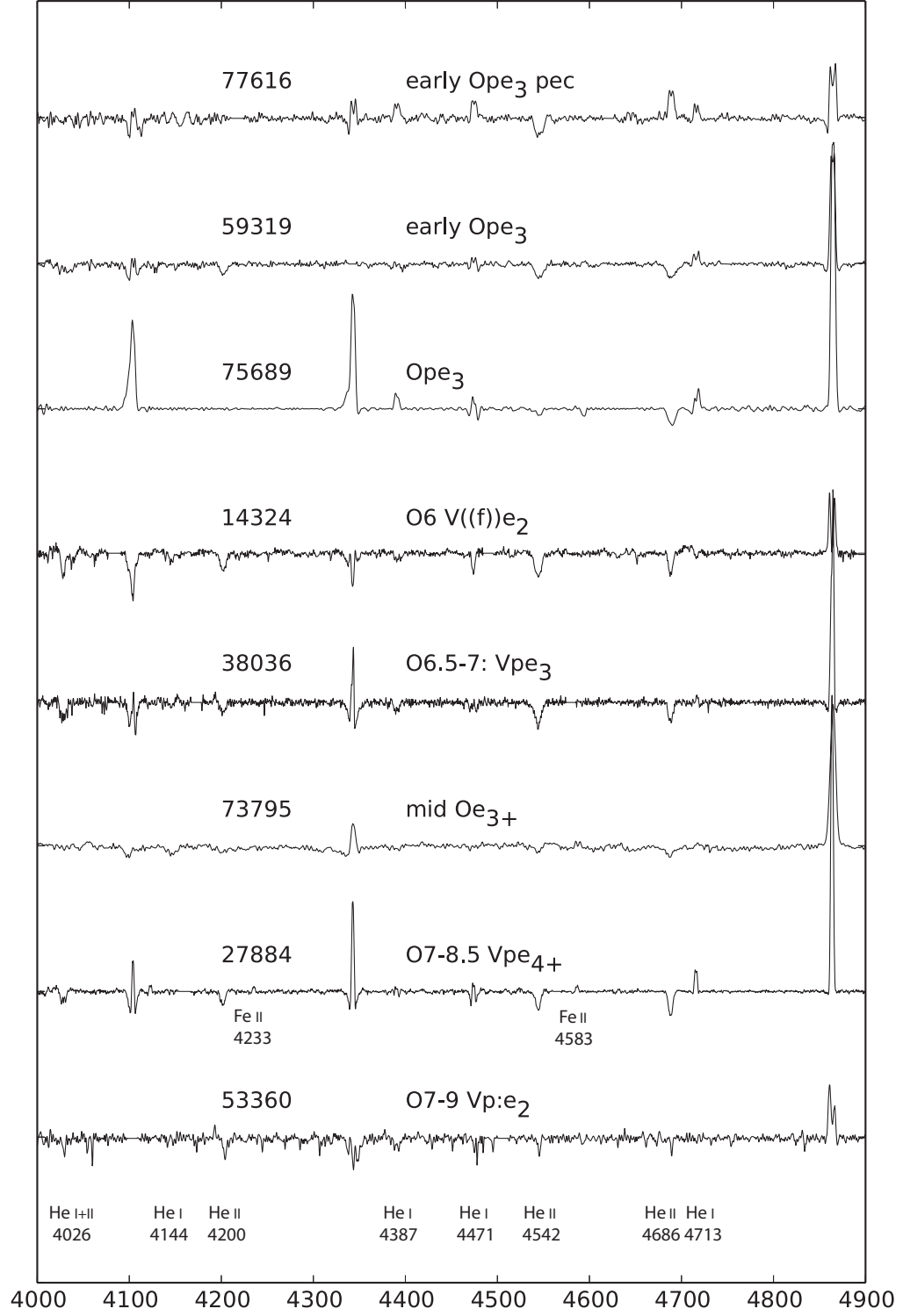


FIG. 7.— Oe/Ope stars with luminosity class V. The Massey (2002) ID numbers and spectral classifications are presented above each spectrum. The absorption lines used to classify these stars are labeled, as well as any He I and Fe II emission lines.



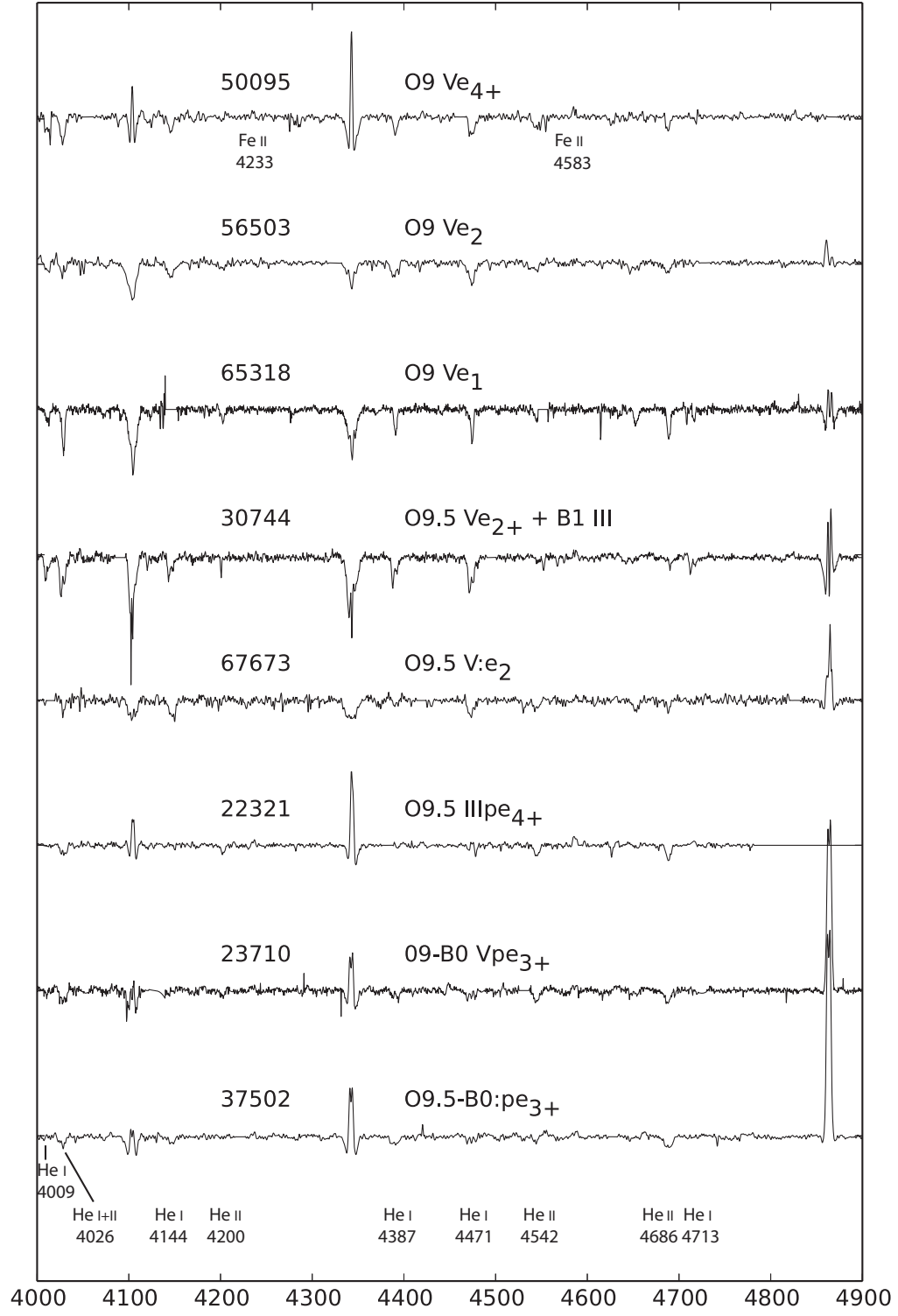


FIG. 7.— continued.

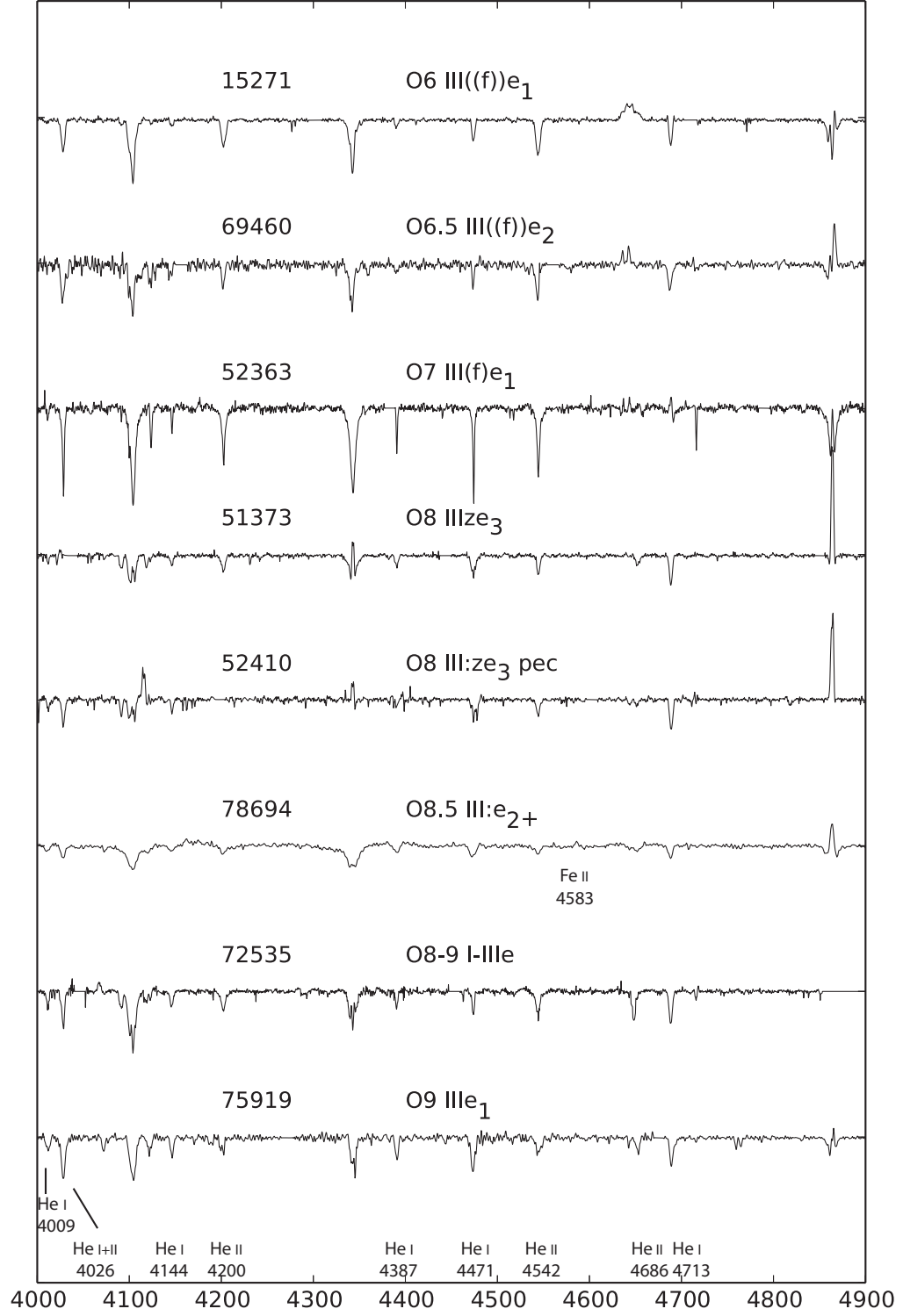


FIG. 8.— Oe/Ope stars with luminosity class III. Star 52410 is peculiar due to the emission feature near H $\delta$ , and star 18329 is peculiar because of the emission feature located near H $\gamma$ . The Massey (2002) ID numbers and our spectral types appear above each spectrum. Absorption features used in classifying these spectra and He I emission lines are labeled.

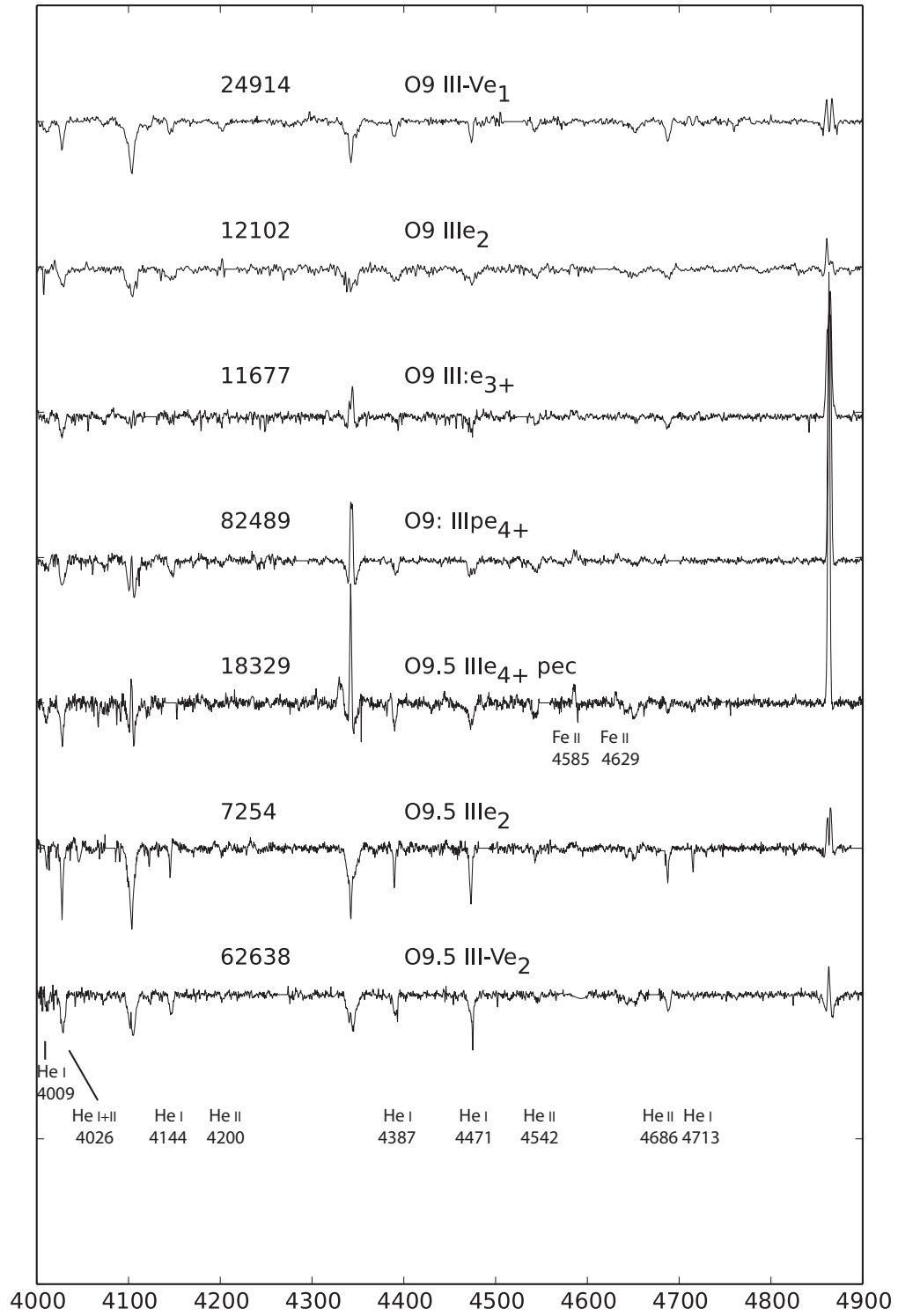


FIG. 8.— continued.